

Influence of the oxidic support material on the platinum-catalyzed benzyl alcohol oxidation

Avela Kunene[†] and Eric van Steen^{*}

Catalysis Institute, Department of Chemical Engineering, University of Cape Town, Private Bag X3, Rondebosch 7701, South Africa; [†] Present address: Helmholtz Zentrum Berlin für Materialien und Energie, Hahn-Meitner-Platz 1, 14109 Berlin, Germany

In honor of Graham Hutchings

Received mm-dd-yyyy

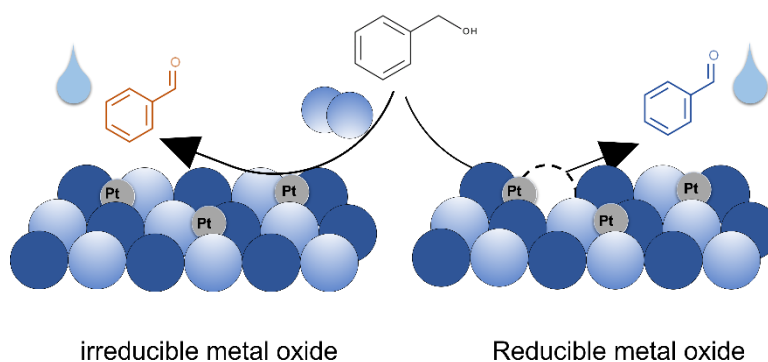
Accepted Manuscript mm-dd-yyyy

Published on line mm-dd-yyyy

Dates to be inserted by editorial office

Abstract

Platinum supported on different oxides is an effective catalyst for the benzyl alcohol oxidation, but the type of support material affects the overall catalytic performance. Here, the performance of dispersed platinum nanoparticles in range of 2.5-4.6 nm supported on reducible oxides (TiO₂(P25), CeO₂, MoO₃ and γ -Fe₂O₃) and an irreducible oxide (γ -Al₂O₃) is investigated for the application of benzyl alcohol oxidation catalysts in the presence of liquid water. The difference in the performance is attributed to the ability of the support to accept hydrogen from benzyl alcohol adsorbed on platinum and the ability to remove surface hydroxyl groups in the form of water.



Keywords: Aerobic, oxidation, benzyl alcohol, platinum, support

Introduction

Heterogeneous catalysis is a surface phenomenon, and as such, the mass-specific catalytic activity decreases with increasing crystallite size of the catalytically active phase.¹ The required high dispersion of the active metal^{2,3} is contrasted by the required particle size to retain catalysts in the reactor and to minimize pressure drop when operating in a packed bed reactor. Hence, the catalytically active material is typically deposited on a support. The support material may, however, play a role beyond dispersing the catalytically active phase by inducing a synergy between the active metal and the support material.⁴⁻⁵

The selective oxidation of alcohols is not different from other reactions and the effect of support material on the oxidation of alcohols has also been observed over Pt, Ir, Pd and Au-based catalysts (see Table 1). The rate of reaction in the benzyl alcohol oxidation, an often-used model reaction,⁶ normalized with respect to the catalytically active metal or metal surface varies easily by an order of magnitude over Pd-⁷, Ir-⁸, Pt-based^{9,10} catalysts (see Table 1). In the oxidation of 3-octanol over gold-based catalysts an almost 30-fold change in the catalytic activity is obtained depending on the support.¹¹ A strong increase in the turnover frequency for the oxidation of benzyl alcohol over iridium supported on titania upon reducing the catalyst at 450 °C instead of 300 °C, was attributed to the presence of a thin titania layer over the catalyst, thus implying an active role of interfacial boundary between the support and the catalytically active metal.⁸

Table 1. Effect of support material on the turnover frequency in the aerobic oxidation of alcohols over supported Pd⁷, Ir⁸, Pt⁹, and Au¹⁰- catalysts

Pd ^{7,i}		Ir ^{8,ii}		Pt ^{9,iii}		Au ^{11,iv}	
Support	TOF, hr ⁻¹	Support	TOF, hr ⁻¹	Support	TOF, hr ⁻¹	Support	TOF, hr ⁻¹
MnO _x	2222	CeO ₂	10	SiO ₂	0	C	15
Mn ₃ O ₄	154	Al ₂ O ₃	35	MgO	1.4	Fe ₂ O ₃	96
CeO ₂	154	TiO ₂	118	Al ₂ O ₃	6.2	TiO ₂	215
Fe ₃ O ₄	197	TiO ₂ -450 ^v	829	TiO ₂	9.5	Nano-CeO ₂	430
				ZnO	13.0		

ⁱ: Benzyl alcohol oxidation at 120 °C, p_{O₂} = 1 bar – no solvent (quasi-turnover frequency); ⁱⁱ: Benzyl alcohol oxidation (1 mol/L in toluene) at 80 °C, p_{O₂} = 1 bar; ⁱⁱⁱ: Benzyl alcohol oxidation (20 mmol/L in water) at 26 °C, p_{O₂} = 0.2 bar; ^{iv}: oxidation of 3-octanol at 80 °C, p_{O₂} = 0.2 bar – no solvent; ^v: reduced in H₂ at 450 °C for 3 hrs.

The turnover frequency (TOF) of a catalytically active metal supported on reducible materials in the oxidation of alcohols appears to be higher than the TOF of the metal supported on an irreducible material, such as carbon or silica. Puigdoller *et al.*¹² and Helali *et al.*¹³ argue that the reducibility of the support affects the overall catalytic performance in the oxidation of alcohols - a reducible oxide may facilitate the oxidation reaction by donating oxygen to an adsorbed species leaving behind an oxygen vacancy sites.¹² Thus, the turnover frequency should correlate with the energy required for the formation of an oxygen vacancy in the support (E_{O,vac}). The activity of platinum-based catalysts in the aqueous phase oxidation of benzyl alcohol⁹ appears to follow the hypothesized trend (see Figure 1; note that the formation energy for oxygen vacancies on γ -Al₂O₃ could not be found and that the data for θ -Al₂O₃ was used here which may have led to the observed discrepancy). However, the activity of iridium-⁸ and gold-¹¹ based catalysts appear to pass a maximum as a function of the energy for the formation of oxygen vacancies in the support (E_{O,vac}), although the maximum

appears to be defined by a single point (the energy of formation for an oxygen vacancy in the different support materials used for palladium-based catalysts⁷ spanned quite a narrow range and a firm conclusion on the dependency of the activity on the formation energy of an oxygen vacancy in the support cannot be drawn yet). This begs the question on whether the activity in the benzyl alcohol oxidation over platinum can be directly correlated with the formation energy of an oxygen vacancy in the oxide support or whether it also passes a maximum as observed for iridium and gold-based catalysts. Hence, here we explore the role of the support in platinum-based catalysts in the aqueous phase oxidation of benzyl alcohol using materials spanning a wide range of $E_{O,vac}$ between -1.74 eV and 6.57 eV.

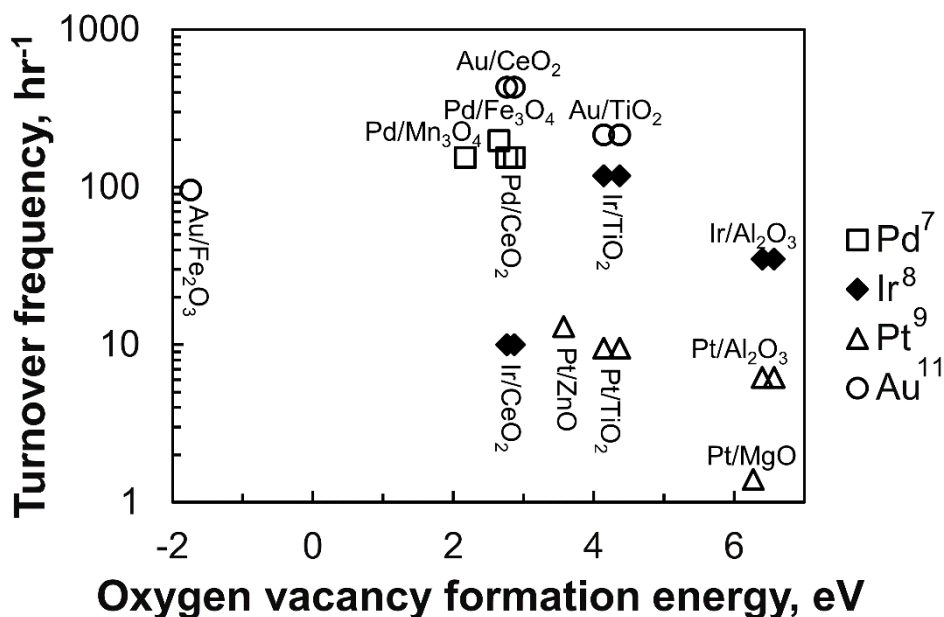


Figure 1. Reported activity^{7-9,11} in the alcohol oxidation (conditions see Table 1) as a function of the energy for the formation of an oxygen vacancy in the support ($E_{O,vac}(\theta\text{-Al}_2\text{O}_3(100)) = 6.57$ eV;¹⁴ $E_{O,vac}(\gamma\text{-Al}_2\text{O}_3(100)) = 6.3$ eV;¹⁵ $E_{O,vac}(\text{MgO}(100)) = 6.27$ eV;¹⁴ $E_{O,vac}(\text{TiO}_2(101)\text{-anatase}) = 4.14$ eV,¹⁴ 4.37 eV;¹⁶ $E_{O,vac}(\text{ZnO}(1010)) = 3.57$ eV;¹⁴ $E_{O,vac}(\text{CeO}_2(111)) = 2.87$ eV,¹⁴ 2.76 eV;¹⁷ $E_{O,vac}(\text{Fe}_3\text{O}_4(111)) = 2.65$ eV;¹⁸ $E_{O,vac}(\text{Mn}_3\text{O}_4(101)) = 2.17$ eV;¹⁹ $E_{O,vac}(\gamma\text{-Fe}_2\text{O}_3(111)) = -1.74$ eV¹⁸).

Results and Discussion

The catalyst support may affect the intrinsic performance of catalysts,^{9,10} and hence platinum supported on different metal oxides (see Table 2) were used as catalysts for the selective oxidation of benzyl alcohol. The supports were selected as they are commonly used supports: $\gamma\text{-Al}_2\text{O}_3$ in particular for oxidation reactions (TiO_2 , CeO_2) displaying a wide range of formation energies of oxygen vacancies (MoO_3 , $\gamma\text{-Fe}_2\text{O}_3$). However, the support may also affect the overall catalyst performance, also through interactions with the fluid phase¹⁹ and the reaction performed in the presence of water showed an improved activity.²¹ Hence, the hydrophobicity/hydrophilicity of the support materials may play a role as well, which was characterized by determining the contact angle with water (as determined using the Washburn method)^{22,23} (see Supporting Information). Molybdenum oxide and maghemite are the most hydrophilic support materials, whereas $\text{TiO}_2(\text{P25})$ and CeO_2 are more hydrophobic.

The activity and selectivity in the benzyl alcohol oxidation may be enhanced due to the presence of Lewis acid sites in the catalyst.^{24,25} Hence, the acidity of the support materials and the catalysts was probed using temperature programmed desorption of ammonia (NH₃-TPD; see Figure S.2) Ammonia is adsorbed on surface acid sites and the amount of ammonia desorbed can be linked to the number of acid sites per unit area. Alumina contains both weak and strong acid sites (the latter characterized by ammonia desorbing at temperatures higher than 450°C) with the latter contributing ca. 33% to the overall number of acid sites. Similarly, γ -Fe₂O₃ also contains weak and strong acid sites (and the latter contributing 22% to the total number of acid sites). Molybdenum oxide only contains strong acid sites, whereas titania (P25) only contains weak acid sites. The amount of ammonia desorbed from CeO₂ was too low to be determined (also a consequence of the low surface area of this material).

Table 2. Surface area, contact angle of water as determined using the Washburn method^{21,21} and the acidity of the support as determined using NH₃-TPD of the used supports.

Support	S _{BET} , m ² /g	$\theta_{\text{contact,water}}$, °	n _{NH₃} , desorbed μmol/g
γ -Al ₂ O ₃ (Puralox SCCa 5-150)	140.5	73.8	809
TiO ₂ (P25)	46.4	80.5	542
CeO ₂	1.7	78.3	0
MoO ₃	3.0	63.5	32
γ -Fe ₂ O ₃	16.2	65.3	89

The support materials were impregnated with an aqueous solution of platinum acid. The obtained catalysts were characterized for the platinum loading, the platinum particle, size distribution, the platinum dispersion, and the acidity of the catalyst (see Table 3). The impregnation of the support materials with platinum acid results in a narrow platinum particle size distribution (an average size between 2.5 and 4.5 nm - see Fig. S.3), which is in reasonable agreement with the obtained average particle diameter from oxygen chemisorption. The acidity of the catalyst was also probed using temperature programmed desorption of ammonia (NH₃-TPD). However, ammonia may also adsorb on platinum. The presence of platinum in the catalyst slightly increases the amount of ammonia desorbing and the NH₃-TPD-spectra of the supported catalysts and the NH₃-TPD-spectra of the support materials do show some differences in the low temperature range (with the exception for Pt/ γ -Fe₂O₃), which may be caused by ammonia previously adsorbed on platinum.

Table 3. Platinum loading, average platinum particle size, platinum dispersion and number of acid sites as determined from NH₃-TPD.

Sample	Pt-loading ^a wt.-%	d _{Pt, TEM} ^b nm	D _{Pt} ^c %	d _{Pt, O₂-chem.} ^d nm	n _{NH₃} , desorbed μmol/g
Pt/TiO ₂ (P25)	3.9	4.6 ± 0.6	30	3.8	882
Pt/ γ -Al ₂ O ₃	4.5	- ^e	42	2.6	605
Pt/CeO ₂	1.7	- ^e	29	4.3	3
Pt/MoO ₃	3.7	3.1 ± 0.6	36	3.6	42
Pt/ γ -Fe ₂ O ₃	4.0	2.5 ± 0.5	45	3.3	252

^a: determined using ICP-OES; ^b: from TEM-images using ImageJ[®] (N>100; see Fig. S.3); ^c: platinum dispersion determined from associative and dissociative oxygen uptake;²⁰ ^d:

$d_{Pt,O_2-chem.} = \frac{113}{D_{Pt(\%)}}$; ^e: in brackets the amount desorbed from bare support; ^f: not determined due to poor contrast (see Fig. S.3)

The activity of the catalysts in the liquid phase, selective oxidation of benzyl alcohol was probed using water as a solvent/dispersant. Water could be a good solvent/dispersant for the selective oxidation of alcohols, as it is inert, and it does not combust (thus minimizing the likelihood for explosions), may enhance O₂-dissociation on Pt(111),²¹ may facilitate transfer of atomic hydrogen,²⁶ and may alter the strength of adsorption of the substrate and products due to solvation effects.²⁷ Water may however retard the reaction if it competes with alcohols for the catalytically active site.²⁸ Performing the reaction using water as a solvent/dispersant may result in a four-phase system with a gas phase, two liquid phases, an aqueous and an organic phase, and a solid phase (the solid catalyst).²⁰ The reduced miscibility of water and benzyl alcohol may also affect the observed activity if the reaction is controlled by external mass transfer. It is thus of importance to see whether the catalyst is preferentially surrounded by the aqueous phase or by the organic phase. Platinum supported on the most hydrophobic TiO₂(P25) oxide support is preferentially surrounded by the organic phase (see Fig. S.4) or at the interface between the aqueous and organic phase. The relatively hydrophilic catalysts Pt/γ-Al₂O₃, Pt/CeO₂ and Pt/MoO₃ are surrounded by both liquid phases. Platinum supported on maghemite (γ-Fe₂O₃) appears to be on the interface of the aqueous/organic phase.

Figure 2 demonstrates the effect of water as a solvent/dispersant on benzyl alcohol oxidation reaction over platinum supported on reducible and irreducible metal oxide support. In the presence of water, a much higher conversion of benzyl alcohol can be obtained than in the absence of water. This is not only attributed to the lower number of moles of benzyl alcohol present in the reactor initially (which decreases from 0.67 mol to 0.27 mol). The initial rate of consumption of benzyl alcohol increases from 5.9 ± 1.4 mmol/g/hr to 37.0 ± 1.0 mmol/g/hr for Pt/TiO₂(P25). Furthermore, it can be observed that the rate of reaction over Pt/TiO₂(P25) decreases significantly with time in the absence of water, implying significant catalyst deactivation. Deactivation is more pronounced in the benzyl alcohol oxidation over Pt/γ-Al₂O₃.

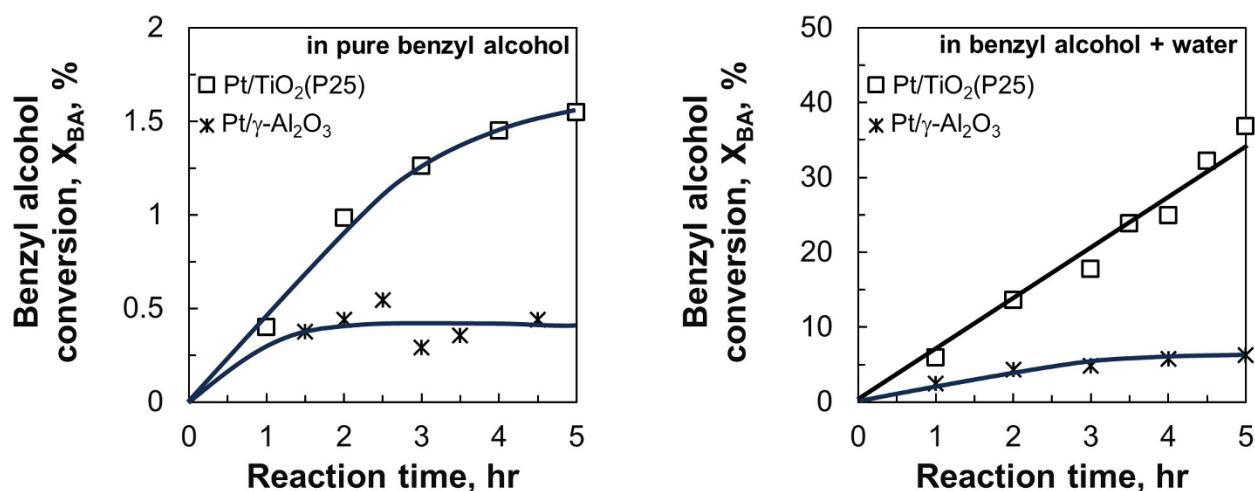


Figure 2. Benzyl alcohol conversion over Pt/TiO₂(P25) and Pt/γ-Al₂O₃ (right) as a function of reaction time in pure benzyl alcohol (left) and in a benzyl alcohol/water mixture containing 7 mol-% benzyl alcohol (right). Conditions: T = 90°C, p = 5 bar, air flow rate = 100 mL_N/min, m_{catalyst} = 0.5 g, V_{liquid} = 70 mL).

Despite the catalyst deactivation, it can be deduced that the initial activity of Pt/γ-Al₂O₃ appears to be less (7.8 ± 0.7 mmol/g/hr) than of Pt/TiO₂, when performing the reaction in the presence of water (catalyst

deactivation appears to be so severe on Pt/ γ -Al₂O₃ when performing the reaction in absence of water that a conclusion on the initial rate of reaction over Pt/ γ -Al₂O₃ can only be poorly estimated). This implies that the turnover frequency over Pt/TiO₂(P25) is 7-8 times higher than over Pt/ γ -Al₂O₃, i.e., a substantially stronger increase than previously reported by Liu *et al.*⁹ who tested their catalysts at 26°C.

The obtained rate of reaction (as determined from the change in the conversion with time) was re-calculated in terms of a turnover frequency. The turnover frequency (TOF) for benzyl alcohol oxidation over Pt/TiO₂(P25) under dry conditions was $26 \pm 5 \text{ hr}^{-1}$, significantly higher than the turnover frequency obtained over Pt/ γ -Al₂O₃ (TOF: $9 \pm 4 \text{ hr}^{-1}$). The difference between the supports becomes even more apparent with the presence of water in the reaction mixture. The turnover frequency improved over both catalysts, but the rate was more enhanced over Pt/TiO₂(P25) ($619 \pm 18 \text{ hr}^{-1}$) than over Pt/ γ -Al₂O₃ (TOF: $80 \pm 7 \text{ hr}^{-1}$). This may hint at some interaction between the support and water affecting the rate of reaction.

The difference in the conversion as a function of time on-line between Pt/TiO₂(P25) and Pt/ γ -Al₂O₃ depicted in Figure 2 was also observed in the benzyl alcohol oxidation over Pt/CeO₂, Pt/MoO₃ and Pt/ γ -Fe₂O₃ (see Figure S.6). Pt/TiO₂(P25) appears to be the most active catalyst, reaching the highest conversion in the oxidation of benzyl alcohol in the presence of water. The conversion obtained over Pt/MoO₃ is somewhat less than the conversion obtained over Pt/TiO₂(P25), but this catalyst is more active than Pt/CeO₂. The obtained conversion over Pt/ γ -Fe₂O₃ appears initially to be like the conversion obtained over Pt/ γ -Al₂O₃, although the former does not appear to deactivate as much. Taking into account the difference in metal loading and metal dispersion, the following order of the observed turnover frequency is obtained: Pt/TiO₂(P25) (TOF: $619 \pm 18 \text{ hr}^{-1}$) > Pt/CeO₂ (TOF: $556 \pm 28 \text{ hr}^{-1}$) > Pt/MoO₃ (TOF: $326 \pm 20 \text{ hr}^{-1}$) > Pt/ γ -Fe₂O₃ (TOF: $99 \pm 4 \text{ hr}^{-1}$) > Pt/ γ -Al₂O₃ (TOF: $80 \pm 7 \text{ hr}^{-1}$). Plotting the obtained turnover frequencies as a function of the energy for the formation of a vacancy in the support, shows clearly the presence of a volcano plot for the activity of platinum-based catalysts in the benzyl alcohol oxidation (see Figure 3), as previously seen for the oxidation of benzyl alcohol over iridium-based catalysts⁸ and the oxidation of 3-octanol over gold-based catalysts.¹¹ The presence of a maximum in the activity as a function of the energy of formation of an oxygen vacancy implies that the reducibility of the support material is not the sole factor at play in determining the activity of the catalyst.

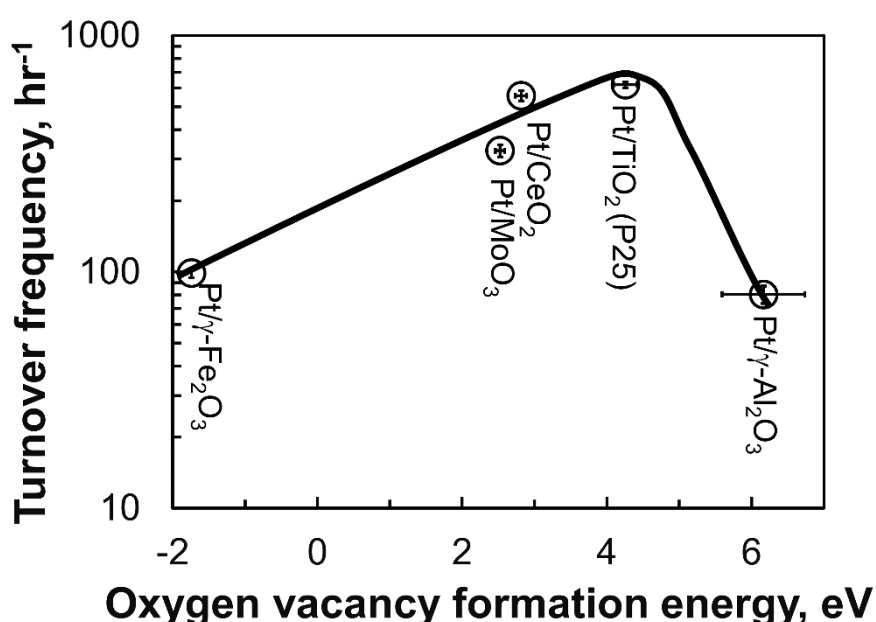


Figure 3. Turnover frequency in the benzyl alcohol conversion over platinum-based catalyst supported on different oxides as a function of the energy for the formation of an oxygen vacancy. Conditions: $T = 90^{\circ}\text{C}$, $p = 5 \text{ bar}$, air flow rate = $100 \text{ mL}_n/\text{min}$, $m_{\text{catalyst}} = 0.5 \text{ g}$, $V_{\text{liquid}} = 70 \text{ mL}$.

The decline in the observed turnover frequency over platinum-based catalysts in the benzyl alcohol oxidation in the presence of water upon changing the support material from $\text{TiO}_2(\text{P25})$ to CeO_2 , MoO_3 and $\gamma\text{-Fe}_2\text{O}_3$ is at odds with the idea that the support donates oxygen to the catalytically active material leaving behind an oxygen vacancy - the energy of formation of an oxygen vacancy is lower on $\gamma\text{-Fe}_2\text{O}_3$ than on oxides, such as TiO_2 , CeO_2 , MoO_3 , but platinum supported on $\gamma\text{-Fe}_2\text{O}_3$ is less active than platinum supported on the other oxides. Furthermore, the donation of oxygen from the support to the platinum surface is quite endothermic (with the exception for the donation of oxygen from $\gamma\text{-Fe}_2\text{O}_3$). For instance, the donation of oxygen from TiO_2 (anatase) to $\text{Pt}(111)$, leaving an oxygen vacancy on TiO_2 , is estimated to be associated with an energy barrier of at least 3 eV.

The oxidation of benzyl alcohol is thought to proceed via transfer of atomic hydrogen to e.g. surface oxygen or surface hydroxyl species, yielding a surface benzyl alkoxide species.^{35,36} The second hydrogen transfer and desorption will lead to the formation of benzaldehyde. The transfer of atomic hydrogen to the dominant surface oxygen species on $\text{Pt}(111)$ ²¹ is thought to be difficult.³⁷ $\text{Pt}(100)$ contains more surface hydroxyl species, in addition to surface oxygen species under reaction conditions,²¹ but hydrogen transfer to surface hydroxyl species is also thought to be associated with a significant energy barrier.³⁷ Hence, the formation of water may become limiting in the oxidation of benzyl alcohol over platinum-based catalysts. The support may assist here in accepting hydrogen from the substrate yielding a surface hydroxyl species on the support (see Figure 4).

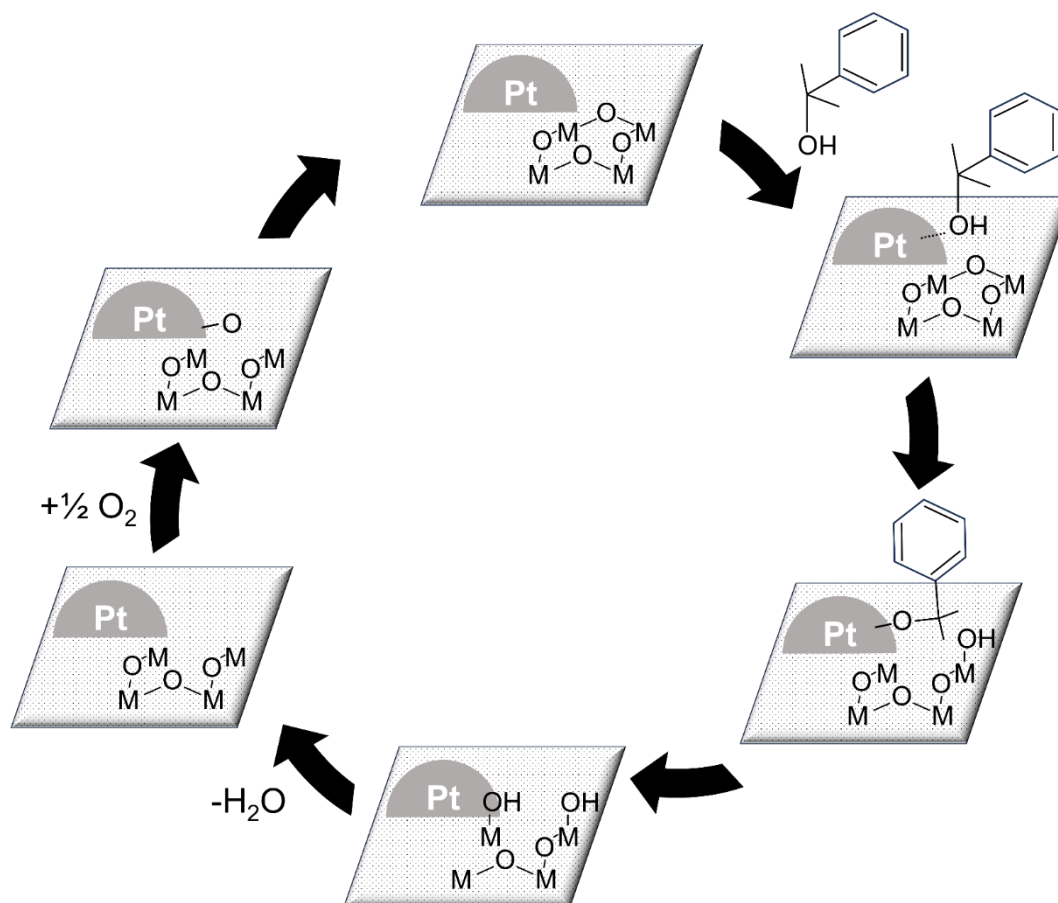


Figure 4. Schematic representation of the role of the support in the oxidation of benzyl alcohol in an oxide support.

The benzyl alcohol oxidation over platinum-based catalysts yields primarily benzyl aldehyde (see Figure 5), with benzaldehyde being the only product obtained over Pt/ γ -Al₂O₃ (albeit at relatively low conversion) and Pt/MoO₃ up to a slightly higher conversion of up to 11%. The more active catalyst, Pt/TiO₂ (P25), shows a 100% selectivity for the formation of benzaldehyde up to a benzyl alcohol conversion of 15–20%, but decreases slightly at higher conversion levels (with a selectivity of larger than 98% at a conversion of up to 40% over Pt/TiO₂ (P25)). The decrease in the selectivity at higher conversions is attributed to the formation of consecutive oxidation product, benzoic acid. The decline in the selectivity for the formation of benzaldehyde with the conversion of benzyl alcohol is stronger on Pt/CeO₂ and Pt/ γ -Fe₂O₃, implying that the ratio of the rate of the secondary conversion of benzaldehyde and the rate of oxidation of benzyl alcohol is higher over these catalysts. It is tempting to correlate the activity for the consecutive oxidation of benzaldehyde with the energy of formation for oxygen vacancies as well. However, the high selectivity for the formation of benzaldehyde obtained over Pt/MoO₃ breaks this correlation. Furthermore, the low selectivity for the formation of benzaldehyde does not appear to correlate with the acidity of the support either.

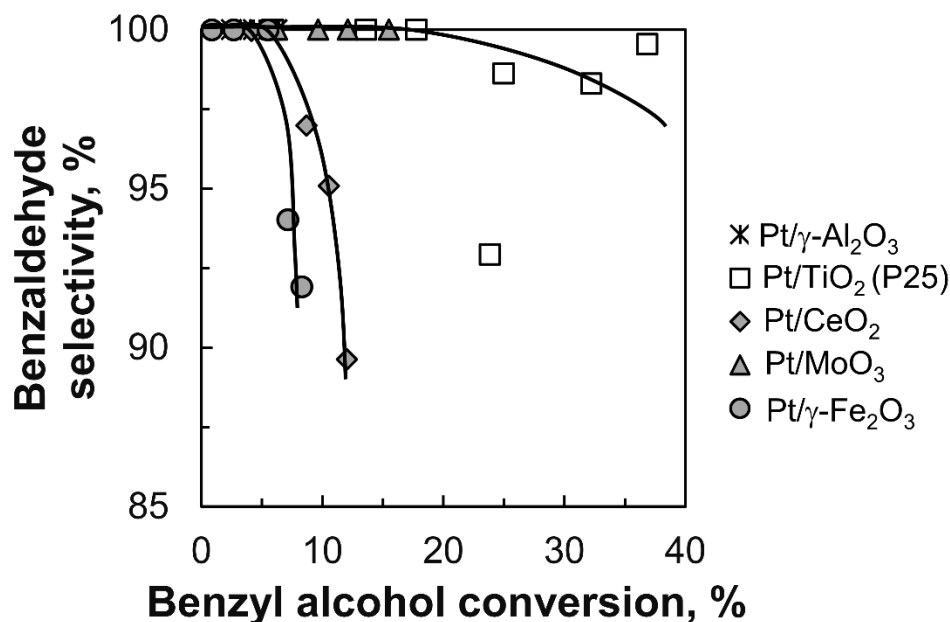


Figure 5. Selectivity for the formation of benzaldehyde as a function of the benzyl alcohol conversion. Conditions: T = 90°C, p = 5 bar, air flow rate = 100 mL_N/min, m_{catalyst} = 0.5 g, V_{liquid} = 70 mL).

Conclusions

The benzyl alcohol oxidation over platinum-based catalysts is accelerated when the reaction takes place in the presence of liquid water. Under these conditions, platinum supported on TiO₂-P25 was the most active catalyst and the selectivity for the formation of formaldehyde was larger than 98% at a conversion of up to 40%. The activity of platinum-based catalysts depends strongly on the choice of the oxidic support material. It is

postulated that this is related to the ability of the support to accept hydrogen from the adsorbed substrate and the removal of so-generated surface hydroxyl groups as water.

Experimental Section

General. The support materials (TiO₂ (P25) – Degussa P25, Evonik, $S_{\text{BET}} = 46.4 \text{ m}^2/\text{g}$; $\gamma\text{-Al}_2\text{O}_3$ – Condea Alumina, Puralox SCCa 5-150, Sasol Technology, $S_{\text{BET}} = 140.5 \text{ m}^2/\text{g}$, MoO₃ – Sigma-Aldrich, $S_{\text{BET}} = 3.0 \text{ m}^2/\text{g}$; CeO₂ – Sigma-Aldrich, $S_{\text{BET}} = 1.7 \text{ m}^2/\text{g}$; $\gamma\text{-Fe}_2\text{O}_3$ – prepared via by precipitation from an aqueous solution of FeCl₃ with an aqueous solution of NaOH drying the precipitate overnight in an oven at 120°C, $S_{\text{BET}} = 16.2 \text{ m}^2/\text{g}$) are calcined in a static oven at 350 °C for 2 hrs, to remove any adsorbing species, e.g. organics whilst in storage. A series of supported platinum catalysts (ca. 4 wt.-% Pt) were prepared by slurry impregnation of an aqueous platinumic acid solution (0.52M) on calcined TiO₂ (P25), $\gamma\text{-Al}_2\text{O}_3$, MoO₃, CeO₂ and $\gamma\text{-Fe}_2\text{O}_3$. The resulting catalyst precursors were calcined in a static oven at 350 °C for 6 hrs.

The elemental composition of the catalysts was verified by inductively coupled plasma-optical emission spectroscopy (ICP-OES) using a Varian ICP 730-ES spectrophotometer. The morphology of the nanoparticles on the supports were imaged using transmission electron microscope (TEM) using a TECHNIA 200II operating at 200kV. The samples were sonicated in methanol for ca. 10 min. Subsequently, the suspension was loaded on a carbon copper coated grid for analysis. The particle size distribution and the average particle size of the nano-sized particles representing the noble metal were determined by measuring ca. 200 nanoparticles using ImageJ®. The platinum dispersion was further determined using O₂-uptake was determined by chemisorption analysis in an ASAP 2020 C unit (Micromeritics). The sample (ca. 150 mg) was evacuated at 110 °C for 30 min. Subsequently, the sample was treated in flowing hydrogen for 12 hrs at 350-400°C and atmospheric pressure followed by evacuation of the sample at the reduction temperature for 120 minutes. The O₂-uptake was determined at 90°C and modelled assuming both associative and dissociative adsorption of O₂.²⁰

Temperature programmed desorption (TPD) of ammonia on a Micromeritics Autochem II was used to determine the acidity of the catalysts. Ammonia was adsorbed on the catalyst by passing a mixture of 5% NH₃ in He (20 mL_n/min) over the sample (ca. 150 mg) at 120°C for 1 h (after degassing for 1 h in helium (20 mL_n/min) at 500°C). Physisorbed ammonia was removed at 120°C by flowing helium (20 mL_n/min) over the sample for 1 h. Subsequently, the temperature of the sample was increased linearly (heating rate: 10°C/min) to 700°C, at which temperature it was kept for 3 hrs. The composition of the effluent was monitored by a thermal conductivity detector (TCD).

The performance of the synthesized platinum-based catalysts in the selective oxidation of benzyl alcohol was tested in a semi-batch reactor system. The synthesized catalyst (0.5 g) was added to a liquid mixture (70 mL) of benzyl alcohol in water (7 mole-%) in a 250 mL autoclave reactor. The stirred autoclave (850 rpm) is purged with nitrogen and heated to 90°C at 10°C/min. At the reaction temperature, the reactor was pressurized to 5 bar whilst continuously passing air (100 mL_n/min) through the reactor. The gas in the outlet passes through a condenser operating at -7°C and 5 bar, to remove condensable vapors. Samples of the liquid phase (1 mL) were collected through the dip tube whilst stirring. The biphasic reaction mixture²⁰ was homogenized by adding methanol to the mixture (and thus the conversion and selectivity can only be determined by internal normalization of the organic product compounds and benzyl alcohol in the sample). The sampling procedure

may have led to some removal of the catalyst from the reactor; to minimize loss in the catalyst mass, sampling was only done hourly for 5 hrs.

Acknowledgements

Financial support from NRF (UID: 93441 and 114606) is gratefully acknowledged.

Supplementary Material

The supplementary material shows contact angle of water with the support materials, the determination of the heat of immersion of the support in water, the NH₃-TPD profiles of the support and the catalysts, TEM-images and particle size distributions of the catalysts, experimental set-up, the benzyl alcohol conversion as a function of reaction time, and the correlation of the adsorption energy of water and the energy of formation of oxygen vacancies for the used support materials.

References

1. Iglesia, E. *Appl. Catal. A Gen.* **1997**, *161*, 59.
[https://doi.org/10.1016/S0926-860X\(97\)00186-5](https://doi.org/10.1016/S0926-860X(97)00186-5).
2. De Beer, M.; Kunene, A.; Nabaho, D.; Claeys, M.; van Steen, E. *J. South. Afr. Inst. Min. Metall.* **2014**, *114*, 157.
<http://www.scielo.org.za/pdf/jsaimm/v114n2/06.pdf>.
3. Tucker, C.L.; van Steen, E. *Catal. Lett.* **2021**, *151*, 2631.
<https://doi.org/10.1007/s10562-020-03475-7>.
4. Tauster, S.J.; Fung, S.C.; Garten, R.L. *J. Am. Chem. Soc.* **1978**, *100*, 170.
<https://doi.org/10.1021/ja00469a029>.
5. Macheli, L.; Carluschi, E.; Doyle, B.P.; Leteba, G.; van Steen, E. *J. Catal.* **2021**, *395*, 70.
<https://doi.org/10.1016/j.jcat.2020.12.023>.
6. Crombie, C.M.; Lewis, R.J.; Taylor, R.L.; Morgan, D.J.; Davies, T.E.; Folli, A.; Murphy, D.M.; Edwards, J.K.; Qi, J.; Jiang, H.; Kiely, C.J.; Liu, X.; Skjøth-Rasmussen, M.S.; Hutchings, G.J. *ACS Catal.* **2021**, *11*, 2701.
<https://doi.org/10.1021/acscatal.0c04586>.
7. Qi, B.; Wang, Y.; Lou, L.L.; Yang, Y.; Liu, S. *React. Kinet. Mech. Catal.* **2013**, *108*, 519.
<https://doi.org/10.1007/s11144-012-0529-y>.
8. Ito, S.; Wang, X.; Waheed, A.; Li, G.; Maeda, N.; Meier, D.M.; Naito, S.; Baiker, A. *J. Catal.* **2021**, *393*, 42-50.
<https://doi.org/10.1016/j.jcat.2020.11.010>.
9. Liu, J.; Zou, S.; Wu, J.; Kobayashi, H.; Zhao, H.; Fan, J. *Chin. J. Catal.* **2018**, *39*, 1081.
[https://doi.org/10.1016/S1872-2067\(18\)63022-0](https://doi.org/10.1016/S1872-2067(18)63022-0).
10. Hong, Y.; Yan, X.; Liao, X.; Li, R.; Xu, S.; Xiao, L.; Fan, J. *Chem. Commun.* **2014**, *50*, 9679.
<https://doi.org/10.1039/C4CC02685C>.
11. Abad, A.; Concepción, P.; Corma, A.; García, H. *Angew. Chem. Int. Ed.* **2005**, *44*, 4066.
<https://doi.org/10.1002/anie.200500382>.
12. Puigdollers, A.R.; Schlexer, P.; Tosoni, S.; Pacchioni, G. *ACS Catal.* **2017**, *7*, 6493.

- <https://doi.org/10.1021/acscatal.7b01913>.
13. Helali, Z.; Jedidi, A.; Syzgantseva, O.A.; Calatayud, M.; Minot, C. *Theor. Chem. Acc.* **2017**, *136*, 100.
<https://doi.org/10.1007/s00214-017-2130-y>.
 14. Hinuma, Y.; Toyao, T.; Kamachi, T.; Maeno, Z.; Takakusagi, S.; Furukawa, S.; Takigawa, I.; Shimizu, K.-i. *J. Phys. Chem. C* **2018**, *122*, 29435.
<https://doi.org/10.1021/acs.jpcc.8b11279>.
 15. Pustovarov, V.A.; Perevalov, T.V.; Gritsenko, V.A.; Smirnova, T.P.; Yelisseyev, A.P. *Thin Solid Films* **2011**, *519*, 6319.
<https://doi.org/10.1016/j.tsf.2011.04.014>.
 16. Li, H.; Guo, Y.; Robertson, J. *J. Phys. Chem. C* **2015**, *119*, 18160.
<https://doi.org/10.1021/acs.jpcc.5b02430>.
 17. Mayernick, A.D.; Janik, M.J. *J. Phys. Chem. C* **2008**, *112*, 14955.
<https://doi.org/10.1021/jp805134s>.
 18. Jian, W.; Wang, S.-P.; Zhang, H.-X.; Bai, F.-Q. *Inorg. Chem. Front.* **2019**, *6*, 2660.
<https://doi.org/10.1039/C9QI00351G>.
 19. Feng, C.; Chen, C.; Xiong, G.; Yang, D.; Wang, Z.; Pan, Y.; Fei, Z.; Lu, Y.; Liu, Y.; Zhang, R.; Li, X. *Appl. Catal., B* **2023**, *318*, 122528.
<https://doi.org/10.1016/j.apcatb.2023.122528>.
 20. Villa, A.; Wang, D.; Dimitratos, N.; Su, D.; Trevisan, V.; Prati, L. *Catal. Today* **2010**, *150*, 8.
<https://doi.org/10.1016/j.cattod.2009.06.009>.
 21. Kunene, A.; van Heerden, T.; Gambu, T.G.; van Steen, E. *ChemCatChem* **2020**, *12*, 4760.
<https://doi.org/10.1002/cctc.202000759>.
 22. Galet, L.; Patry, S.; Dodds, J. *J. Colloid Interface Sci.* **2010**, *346*, 470.
<https://doi.org/10.1016/j.jcis.2010.02.051>.
 23. Taguta, J.; O'Connor, C.T.; McFadzean, B. *Colloids Surfaces A, Physicochem. Eng. Asp.* **2018**, *558*, 263.
<https://doi.org/10.1016/j.colsurfa.2018.08.059>.
 24. Wu, P.; Song, L.; Wang, Y.; Liu, X.; He, Z.; Bai, P.; Yan, Z. *Appl. Surf. Sci.* **2021**, *537*, 148059.
<https://doi.org/10.1016/j.apsusc.2020.148059>.
 25. Ramesh, A.; Manigandan, R.; Mohamad Ali, B.; Dhandapani, K.; Thi Da, C.; Nguyen-Le, M.-T. *J. Alloys Compd.* **2022**, *918*, 165729.
<https://doi.org/10.1016/j.jallcom.2022.165729>.
 26. Mahlaba, S.V.L.; Hytoolakhan Lal Mahomed, N.; Govender, A.; Guo, J.; Leteba, G.M.; Cilliers, P.L.; van Steen, E. *Angew. Chem. Int. Ed.* **2022**, *61*, e202206841.
<https://doi.org/10.1002/anie.202206841>
 27. Frassoldati, A.; Pinel, C.; Besson, M. *Catal. Today* **2011**, *173*, 81.
<https://doi.org/10.1016/j.cattod.2011.02.058>.
 28. Tatsumi, H.; Liu, F.; Han, H.-L.; Carl, L.M.; Sapi, A.; Somorjai, G.A. *J. Phys. Chem. C* **2017**, *121*, 7365.
<https://doi.org/10.1021/acs.jpcc.7b01432>.
 29. Hass, K.C.; Schneider, W.F.; Curioni, A.; Andreoni, W. *J. Phys. Chem. B* **2000**, *104*, 5527.
<https://doi.org/10.1021/jp000040p>.
 30. Martinez-Casado, R.; Mallia, G.; Harrison, N.M.; Pérez, R. *J. Phys. Chem. C* **2018**, *122*, 20736.
<https://doi.org/10.1021/acs.jpcc.8b05081>.
 31. Fronzi, M.; Piccinin, S.; Delley, B.; Traversa, E.; Stampfl, C. *Phys. Chem. Chem. Phys.* **2009**, *11*, 9188.
<https://doi.org/10.1039/B901831J>.

32. Head, A.R.; Gattinoni, C.; Trotochaud, L.; Yu, Y.; Karslıoğlu, O.; Pletincx, S.; Eichhorn, B.; Bluhm, H. *J. Phys. Chem. C* **2019**, *123*, 16836.
<https://doi.org/10.1021/acs.jpcc.9b03822>.
33. Ntallis, N.; Peyre, V.; Perzynski, R.; Dubois, E.; Trohidou, K.N. *J. Magn. Magn. Mater.* **2019**, *484*, 74.
<https://doi.org/10.1016/j.jmmm.2019.03.132>.
34. Tilocca, A.; Selloni, A. *J. Phys. Chem. B* **2004**, *108*, 4743.
<https://doi.org/10.1021/jp037685k>.
35. Savara, A.; Chan-Thaw, C.E.; Rossetti, I.; Villa, A.; Prati, L. *ChemCatChem* **2014**, *6*, 3464.
<https://doi.org/10.1002/cctc.201402552>.
36. Sankar, M.; Nowicka, E.; Tiruvalam, R.; He, Q.; Taylor, S.H.; Kiely, C.J.; Bethell, D.; Knight, D.W.; Hutchings, G.J. *Chem. Eur. J.* **2011**, *17*, 6277.
<https://doi.org/10.1002/chem.201003484>.
37. Li, K.; Li, Y.; Wang, Y.; He, F.; Jiao, M.; Tang, H.; Wu, Z. *J. Mater. Chem. A* **2015**, *3*, 11444.
<https://doi.org/10.1039/C5TA01017A>.

This paper is an open access article distributed under the terms of the Creative Commons Attribution (CC BY) license (<http://creativecommons.org/licenses/by/4.0/>)